

# VISUALISATION OF TENSOR TIME DOMAIN ELECTROMAGNETIC DATA

T.G. CALDWELL AND H.M. BIBBY

IGNS, Wellington, NZ

**ABSTRACT** - Long Offset Time Domain Electromagnetic (**LOTEM**) measurements traditionally use a single current source. By using a second source, a tensor analysis technique analogous to that used in **DC** resistivity multiple-source bipole-dipole surveying, is possible. An instantaneous apparent resistivity tensor is defined as the relationship between the time varying (total) electric field and the **DC** half space current density vectors due to each source. If the sources are dipoles the three coordinate invariant apparent resistivities of the tensor are independent of source orientation. For a uniform half space, one of the invariants is virtually constant in time, deviating from the half space resistivity by a maximum of 6%. This method provides a way in which the complicated data set obtained during a tensor **LOTEM** survey can be presented in a compact and intelligible form, and has many advantages over conventional methods of analysing **LOTEM** data particularly where the resistivity distribution is three dimensional (**3D**). Results from a **3D** resistivity model of an idealised geothermal reservoir and outflow structure are used to illustrate the power of this analysis.

## INTRODUCTION

The usefulness of any definition of apparent resistivity depends upon how well this parameter reflects the subsurface resistivity distribution. It is usual to choose as the apparent resistivity a parameter that, for a uniform resistivity half space, has the same value as the resistivity of the half space. In more complicated situations the value of the apparent resistivity may only be indirectly related to the resistivity in the earth. A good example is the Schlumberger apparent resistivity which for a uniform half space is equal to the resistivity of the ground. For a horizontally layered structure, however, the apparent resistivity approaches the resistivity of a particular layer only if both the depth to the top of the layer is much less than the current electrode spacing and the layer thickness is much greater than the spacing. In this case the Schlumberger apparent resistivity (as a function of electrode spacing) can be considered to be a low pass filtered version of the resistivity layered structure as a function of depth.

For multiple-source bipole-dipole resistivity surveys the DC apparent resistivity tensor is a useful way of presenting the results of multiple source resistivity surveys even in the case where the resistivity distribution is three dimensional (Bibby 1977, 1986; Bibby and Hohmann 1993). In the cases considered by Bibby and Hohmann (1993) the main features of a **3D** resistivity structure can be discerned directly from maps of either coordinate invariant apparent resistivities or maps showing the apparent resistivity ellipses at each measurement site (see Fig. 1). This method of data presentation is now used routinely in our analysis of multiple source bipole dipole data and serves as the starting

point for subsequent interpretation that may require detailed **2D** or **3D** computer modelling of the results (eg Risk *et al.*, 1993, 1994).

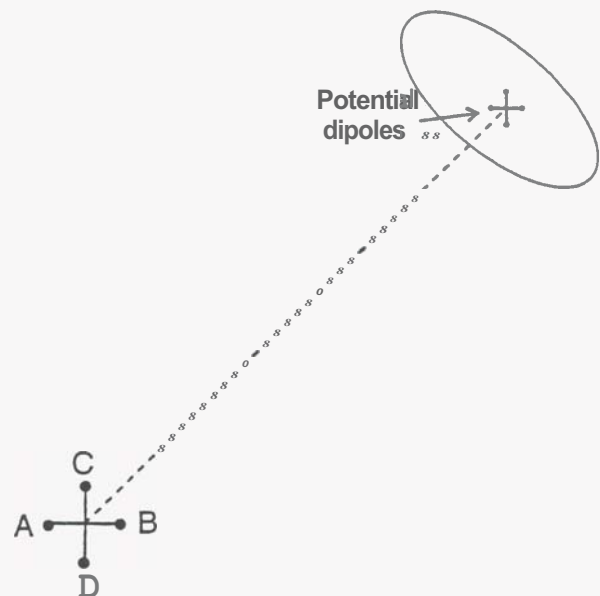


Figure 1: Multiple-source bipole-dipole array. The transmitter array consists of the two perpendicular bipoles AB and CD. At a point P distant from the transmitter bipoles the electric fields due to each bipole are measured using a pair of (very small) orthogonal dipoles. The apparent resistivity tensor, which can be represented by an ellipse, is determined from measurements of the total electric field vectors, the geometry of electrode array and the currents injected in each bipole (Bibby 1977, 1986).

The detection depth of a multiple-source bipole-dipole survey depends upon the distance of the station to the transmitter. In a horizontally layered half space the components of the apparent resistivity tensor in a polar coordinate system are simply the Schlumberger (equivalent to the equatorial dipole) and polar-dipole apparent resistivities (Bibby 1986). The effect of the lateral and vertical resistivity variations are therefore inextricably linked and careful interpretation is needed in order to distinguish the effects of the deeper structure from variations in the near surface resistivity. Applications of this technique in New Zealand have always been complemented by extensive (shallow detection depth) Schlumberger apparent resistivity surveys conducted prior to the bipole-dipole survey. The availability of this data has played an important part in the successful application of the multiple source bipole-dipole technique in New Zealand.

In time domain electromagnetic methods (**TEM** or **TDEM**) the detection depth depends on the time interval between the transmitter pulse and the instant at which the EM fields are measured. In principle both the near surface and deep resistivity structure can be determined at each measurement site. In contrast a bipole-dipole survey produces measurements with a detection depth dependant on the distance between the site and the transmitter. The deep structure is inferred from measurements made over a range of distances.

## LOTEM

The multiple-source bipole-dipole technique (shown in Fig. 1) may be extended to make use of the transient part of the waveform recorded during the measurement of DC resistivities. Since the range between the receiver and transmitter is usually large or has a 'long offset' the technique which uses these transients has become known by the acronym '**LOTEM**'. In this method the transient part of the signal, explicitly ignored in a DC survey, is used to produce a **TEM** sounding at each site. Fig. 2 shows a graph of the electric field produced by grounded dipole on the surface of a uniform resistivity half space as function of time. The transient signal is sensitive to resistivity changes at increasingly greater depths as time increases.

As we have pointed out previously (Caldwell and Bibby, 1993) the physics of the controlled source magneto-telluric (**CSMT**), **LOTEM** and DC resistivity bipole-dipole techniques are closely related; the transmitter and receiver geometry are essentially identical. The differences between these methods occurs in the analysis techniques used and the components of the EM field measured. At late times, or in the frequency domain at long periods, the total electric fields measured in a **LOTEM** or **CSMT** survey must asymptotically approach the DC bipole-dipole values.

As a first step in interpreting data from a **LOTEM** survey it has been traditional to calculate the 'early' and 'late' time apparent resistivities. These parameters, as their names suggest, are defined by the asymptotic behaviour of the transient electric field at veryshort and very long times

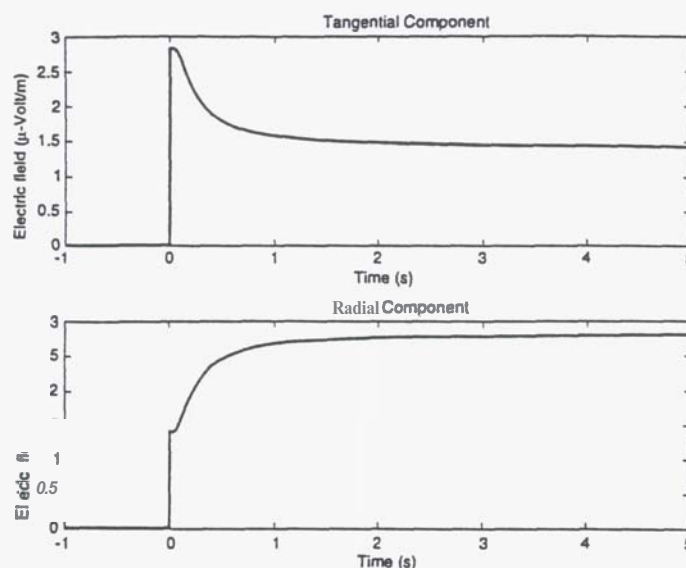


Figure 2: Graphs showing the time dependence of the total electric field due to a grounded dipole source lying on the surface of a  $100 \Omega\text{m}$  half space. The dipole is aligned in the  $x$  direction and has a moment of  $20 \times 10^3$  Amp-m. The field components shown, were calculated for a point 10 km and at an angle of  $45^\circ$  from the transmitter dipole. The figure shows the components in the tangential (a) and radial (b) directions respectively.

after the current is switched. These asymptotic forms are used because, unlike DC resistivity, the magnitude of the electric field in a uniform earth is not linearly dependent on the resistivity of the half space but is a function of both the resistivity and time. Although at early times the asymptotic relationship becomes linear, at late times the transient electric field is inversely proportional to the square root of the resistivity. In the transitional period neither of these apparent resistivities accurately reflect the subsurface resistivity. The ambiguity in deciding the period of applicability for each apparent resistivity together with the habit of plotting both parameters on the same graph has led to the misapprehension that the apparent resistivity in **TDEM** surveys is 'double valued'. The behaviour of these parameters makes them unsuitable for the creation of images of the subsurface resistivity structure

Images of the subsurface derived previously from single source **LOTEM** surveys (Strack 1991 and 1992) have used the resistivity values determined from a 1D inversion of measured data. Although this approach will work well where the resistivity distribution is approximately 1D in more complex situations this approach will not necessarily provide a realistic picture of the subsurface resistivity structure especially if only a single current source is used. When the inductive component of the measured electromagnetic fields is small; the apparent resistivity values may not reflect the subsurface resistivity distribution producing 'false anomalies'. Such anomalies are also characteristic of single source bipole-dipole surveys where the apparent resistivity is strongly dependant on source orientation.

Although the problems associated with using a single current source have been **recognised** for many years in DC surveying' the advantages of multiple sources in **LOTEM** surveys do not appear to have been recognised. The purpose of **this** paper is to introduce a new way of analysing the electric fields measured in a multiple-source **LOTEM** survey that is both simple to apply and provides a mechanism of visualising the results of multiple-source **LOTEM** surveys directly. **This** analysis also makes the relationship to the DC multiple-source bipole method explicit **as well as** making clear the advantages of using more than one source polarisation in **LOTEM** surveys.

## INSTANTANEOUS APPARENT RESISTIVITY TENSOR

**As** a simple extension to the DC apparent resistivity tensor we define the 'instantaneous apparent resistivity tensor' **as**:

$$\underline{E}(t) = \underline{\rho}(t) \underline{J}$$

where  $\underline{E}(t)$  is the electric field vector, due to a current step switched on at  $t=0$  and where  $\underline{J}$  is the DC current density that would be produced in a uniform half space by the same grounded bipole. It is emphasised that the vector field  $\underline{J}$  is simply a normalisation factor that has been chosen to be constant in time. **Thus**  $\underline{\rho}(t)$  is an apparent resistivity tensor defined at each instant  $t$ .

In a Cartesian coordinate system we can represent the four components of the tensor **as** the **matrix**:

$$\underline{\rho}(t) = \begin{bmatrix} \rho_{xx}(t) & \rho_{xy}(t) \\ \rho_{yx}(t) & \rho_{yy}(t) \end{bmatrix}$$

The tensor is determined at each station by recording the time varying components of the total electric field produced by two non-parallel bipole sources. In a Cartesian coordinate system, with (non parallel) bipole sources AB and CD the components of the tensor are given by the solution to the matrix equation:

$$\begin{bmatrix} E_x^{AB}(t) & E_x^{CD}(t) \\ E_y^{AB}(t) & E_y^{CD}(t) \end{bmatrix} = \begin{bmatrix} \rho_{xx}(t) & \rho_{xy}(t) \\ \rho_{yx}(t) & \rho_{yy}(t) \end{bmatrix} \begin{bmatrix} J_x^{AB} & J_x^{CD} \\ J_y^{AB} & J_y^{CD} \end{bmatrix}$$

For uniform half-space of resistivity  $\rho$  the components of the apparent resistivity tensor for dipole sources take the **form**:

$$\underline{\rho}(t) = \begin{bmatrix} 1+f(r/\delta)[2\sin^2\theta - \cos^2\theta]/2, & -3\sin\theta\cos\theta f(r/\delta)/2 \\ -3\sin\theta\cos\theta f(r/\delta)/2, & 1+f(r/\delta)[2\cos^2\theta - \sin^2\theta]/2 \end{bmatrix}$$

where  $\delta$  is a parameter with the dimensions of distance given by  $\delta = (4\rho t/\mu_0)^{1/2}$  (this parameter is  $\sqrt{2}$  times the 'diffusion depth'  $\delta_{TD}$  given in Spies and Frischknecht (1991),  $(r, \theta)$  is the position of the measurement station

from the center of transmitter dipoles in polar coordinates,  $t$  is the time after the current switch, and  $\mu_0$  is the free space magnetic permeability. The function  $f(r/\delta)$  is the general expression for the time dependent part of the total electric field on surface of a uniform half space and is given by the equation:

$$f(r/\delta) = I_{ds} [ \text{erf}(r/\delta) - (4/\pi)^{1/2} (r/\delta) \exp(-r^2/\delta^2) ] / (2\pi^3)$$

where  $I_{ds}$  is the dipole moment.  $f$  depends implicitly upon the resistivity  $\rho$  of the half space and time (Spies and Frischknecht 1991). Providing the sources can be approximated by infinitesimal dipoles then the tensor invariants **are** independent of source orientation (see Bibby, 1994).

## PROPERTIES OF THE TENSOR IN A UNIFORM HALF SPACE

In a polar coordinate system the **off** diagonal components of the tensor vanish and the tensor takes the simple form:

$$\underline{\rho}(t) = \rho \begin{bmatrix} 1-f(r/\delta)/2 & 0 \\ 0 & 1+f(r/\delta) \end{bmatrix}$$

A good way of visualising the behaviour of the tensor **as** a function of time is to examine the behaviour of the apparent resistivity ellipse **as** a function of time. At early times,  $f(r/\delta)=1$ , and the tensor is represented by an ellipse with its major and minor axes oriented tangentially and radially to the sources and with lengths  $2\rho$  and  $\rho/2$  respectively. **As** time increases the ellipse evolves smoothly into a circle of radius  $\rho$ , the DC case. The remarkable thing about this formulation is that the area of the apparent resistivity ellipse remains almost unchanged. **This** behaviour is most easily expressed in **terms** of the invariants.  $P_1$ ,  $1/2$  the trace of the tensor matrix, and  $P_2$ , the square root of the **matrix determinant**, (Bibby 1986).  $P_2$ , which is the radius of the circle with an area equal to that of the apparent resistivity ellipse, is almost constant with time and equal to  $\rho$ . The maximum difference between  $P_2$  and  $\rho$  is about 6% and occurs when  $r/\delta = 1.09$ . At both early **and** late times  $P_2$  approaches  $\rho$ . The limiting values of the invariant  $P_1$  at early and late times are:  $1.5\rho$  and  $\rho$  respectively. The third invariant  $P_3$ , the skew **of** the tensor, is zero.

In **summary**, the instantaneous apparent resistivity **tensor**, which is a **normalisation** of the time varying electric fields by the DC current density, provides invariant parameters (apparent resistivities) which are independent of coordinate and source orientation. One of these invariants,  $P_2$ , is virtually constant in time and deviates from the half space resistivity **by** no more than about .6%. In contrast, the early and late time apparent resistivities traditionally **used** diverge rapidly outside their (limited) **range** of applicability. It important **to** emphasise that to use the tensor formulation requires **information** from more than one source polarisation.



## PROPERTIES OF THE TENSOR IN A LAYERED HALF SPACE

In a layered half space symmetry considerations require that for dipole sources the instantaneous apparent resistivity tensor will be diagonal in a polar coordinate system centred on the source dipoles. Thus, where the resistivity distribution is 1D the invariant  $P_3=0$  at all times. At early times the apparent resistivity ellipse will be identical to that observed for a **uniform** half space with the resistivity of the top layer. At late times the instantaneous apparent resistivity will approach the **DC** apparent resistivity tensor. In a polar coordinate system the **DC** apparent resistivity is given by:

$$\underline{\rho} = \rho_s(r) \begin{pmatrix} 1 - 1/2(r/\rho_s)(d\rho_s/dr) & 0 \\ 0 & 1 \end{pmatrix}$$

where  $\rho_s(r)$  is the Schlumberger apparent resistivity at a spacing  $r$  (see Bibby 1986). This link between the **DC** and **LOTEM** method suggests that the maximum detection depth in a **LOTEM** survey is independent of time and is determined by the distance of the receiver **from** the source as it is in the DC resistivity case.

Fig. 3 shows the behaviour of  $P_2$  as two distance-time 'pseudo sections' for a three layer model. In Fig. 3a data **are shown** for a line a minimum distance of 7.4 km from the current sources while for Fig. 3b the line of measurements is along a radius from the source. For Fig. 3a the distance of the measurement points **from** the source bipoles does not vary significantly and the  $P_p$  pseudo section provides a realistic image of the layered structure. In a **similar** manner to a Schlumberger resistivity sounding, the instantaneous apparent resistivity does not reach the value of the resistivity of the middle layer before the higher resistivity beneath is sensed and apparent resistivity values increase again.

The effect of the change in distance **from** the source can be seen in both profiles. In the centre of Fig. 3a, where the source is nearest to the profile, the contour dips down. The same effect is more clearly shown in Fig. 3b where the measurement points approach the current source. When close to the source, the apparent resistivity at large times **does** not detect the deeper layer and the values reflect the resistivity of the middle layer rather the underlying higher resistivity. **As** the distance from the source becomes greater the value of  $P_p$  at late times increases **as** the underlying higher resistivity layer is sensed. If the profile was extended to greater distances  $P_p$  would eventually reach the resistivity of the bottom layer.

The pseudo section for layered models is similar in many ways to a seismic reflection section where the vertical time axis is indirectly related to depth. Just **as** in the seismic case different layers have different velocities, the diffusion velocity of the EM fields will depend on the resistivity of the layers with low diffusion velocities in low resistivity

and **high** diffusion velocities in high resistivity. In order to convert times to depths we would need, in the language of the seismic processing industry, to 'migrate' the distance-time section into a distancedepth section.

Fig 3a

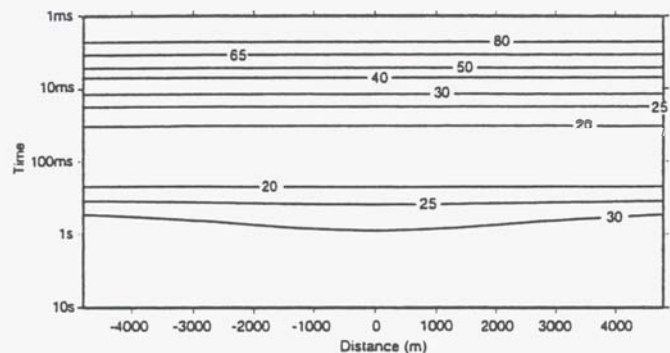


Fig 3b

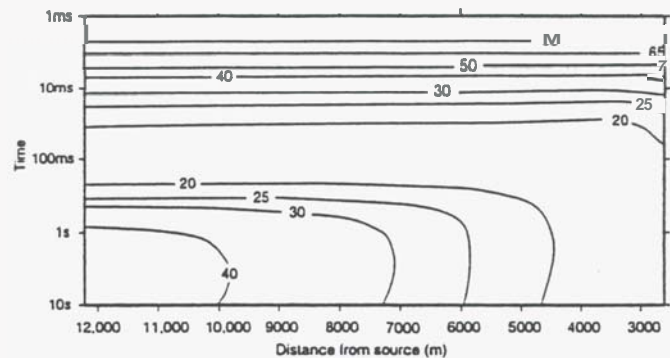


Figure 3: Pseudo sections showing the  $P_2$  invariant of the instantaneous apparent resistivity tensor for a 3 layer model. The contour interval is approximately logarithmic with 10 contours per decade. Layer thicknesses and resistivities for the model were: top layer:  $\rho=100\Omega m$ , thickness = 500m; middle layer  $\rho = 10 \Omega m$ , 1500m thick and a substratum of  $\rho=300\Omega m$ . Fig. 3a shows the pseudo section for a profile centred 7.4 km **from** the common mid point of two perpendicular bipole sources 1 km long. Fig. 3b shows a similar pseudo-section also centred 7.4 km from the bipoles but running away **from** the sources **from** right to left ie the right hand side of the profile is 2.6 km **from** the midpoint of the bipoles.

## PROPERTIES OF THE TENSOR IN A 3D SITUATION

### The 3D Model

The benefits of using more than one source polarisation in DC resistivity surveys are greatest where the resistivity distribution is 3D (Bibby and Hohmann 1993). The **3D** model shown in Fig. 4 is a representation of the resistivity structure of a geothermal reservoir with an associated **outflow** of geothermal fluid. This model was chosen because of the increasing need in **New Zealand** to be able to distinguish upflow and outflow zones. Furthermore **as** exploitation moves to deeper levels improved resistivity images of the deeper parts of the geothermal reservoir and their surroundings will be needed.

The resistivity values **used** are based upon the resistivity structure of the **Ohaaki** geothermal system inferred **from** bipole-dipole surveys (Bibby 1978). **This** model **is** broadly similar to the model used in Pellerin *et al.*(1992) **to** evaluate the detectability of a reservoir or 'upflow zone' lying beneath **a** more extensive area of low resistivity. The conclusion of the Pellerin *et al.*(1992) study of several different EM techniques **was** that only the LOTEM and MT methods are capable of detecting an underlying reservoir in this case. In all cases the **3D** dimensional effects dominate the response and the signal due to the underlying reservoir is very weak. **A** similar modelling study conducted by ourselves (Caldwell and Bibby, 1993) showed that a DC multiple-source bipole-dipole survey would also detect the reservoir. **Also** our study showed that the small signal due to the underlying low resistivity reservoir is dominated by the effects of the horizontal boundaries of the low resistivity **body** representing the reservoir.

#### The method

The instantaneous apparent resistivities, shown in Fig. 5 as **a** series of pseudo sections, were calculated from electric fields computed using the **3D** integral equation modelling method described in Xiong (1992) and Xiong and Tripp (1995). The fields were computed at 25 values of  $t$ , logarithmically spaced between **1 ms** and **10 s**. Electric field vectors for each source were calculated at 200m intervals along the **9.6 km** profile, **AA'**, as shown in Fig. 4. All the computations were undertaken using **a DEC Alpha 3000** computer.

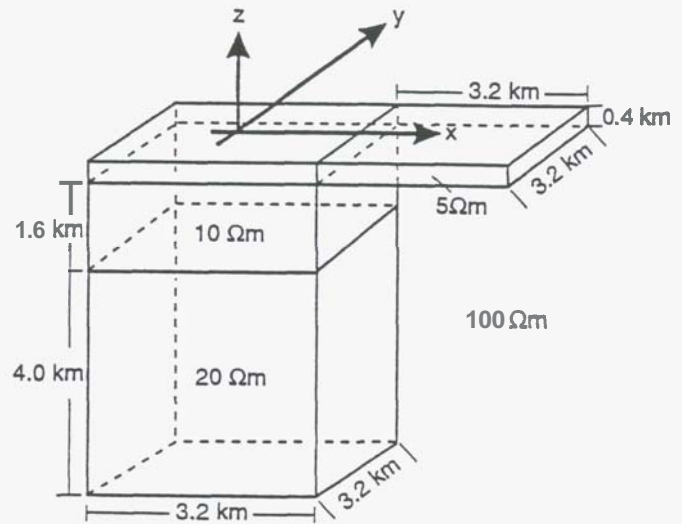
#### Results

Results are presented for **4** different transmitter sites, marked **S1** to **S4** in Fig. 4b., each **7.4 km** **from** the center of the reservoir. **Two** apparent resistivity invariants,  $P_2$  and  $\rho_{min}$ , have been used **to** illustrate the modelling results. The invariant  $P_2$  is a measure of the area of the apparent resistivity ellipse and **as** such it is less sensitive to the effects of lateral resistivity changes than invariants that are more directly related to the orientation and shape of the ellipse. The length of the minor **axis** of the ellipse,  $\rho_{min}$ , provides **a** more sensitive indicator of lateral resistivity changes in **this** case.

For each of the current source locations shown in Fig. 4, both the outflow and upflow zones can be identified in Fig. 5 **by** using **a** combination of the plotted parameters,  $P_2$  and  $\rho_{min}$ , although the pattern of apparent resistivity varies in detail with the position of the transmitter. The clearest image of the reservoir is obtained when the outflow tongue is furthestmost **from** the transmitter ( $P_2$ , Fig. 5a). **As** the transmitter is rotated around the reservoir (Fig. 5a, 5c, 5e, and 5g) the image provided by the  $P_2$  invariant becomes less distinct. However, the effect of the reservoir on the  $\rho_{min}$  pseudo sections (Fig. 5b, 5d, 5f, and 5h) tends to **compensate** for the loss of resolution in  $P_2$ . These pseudo sections **also** provide the clearest image of the higher resistivity beneath the outflow structure. **This** parameter **will** be more strongly influenced by the lateral boundary of

the deeper reservoir, which will enhance the contrast in  $\rho_{min}$  beneath the outflow structure. The occurrence of a small peak in the apparent resistivity near **this** edge of the reservoir, best seen in Fig. 5f, illustrates **this** point.

#### (a) Perspective view



#### (b) Map view

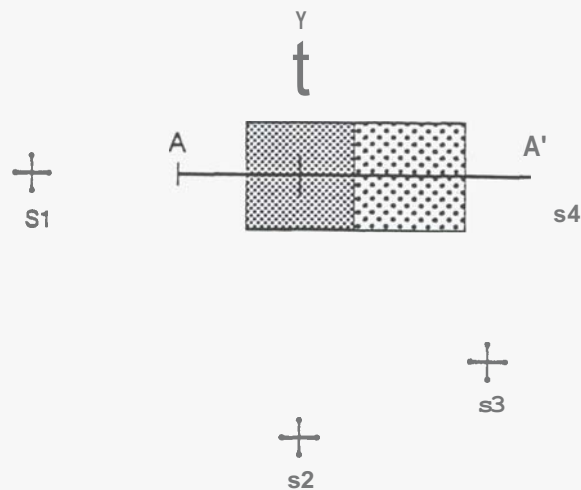


**Figure 4:** Three dimensional resistivity model of an idealised geothermal system and associated outflow tongue. The geothermal reservoir or upflow zone is represented by the 10 and 20  $\Omega m$  bodies. The 5  $\Omega m$  body represents the upper part of the reservoir and an outflow in the  $x$  direction. A perspective view of the model is shown in Fig. 4a. The map view, Fig. 4b, shows the 4 different sets of sources, labelled S1 to S4, used for the results presented in Fig. 5. Each of these sources is 7.4 km, horizontally, from the centre of the reservoir.

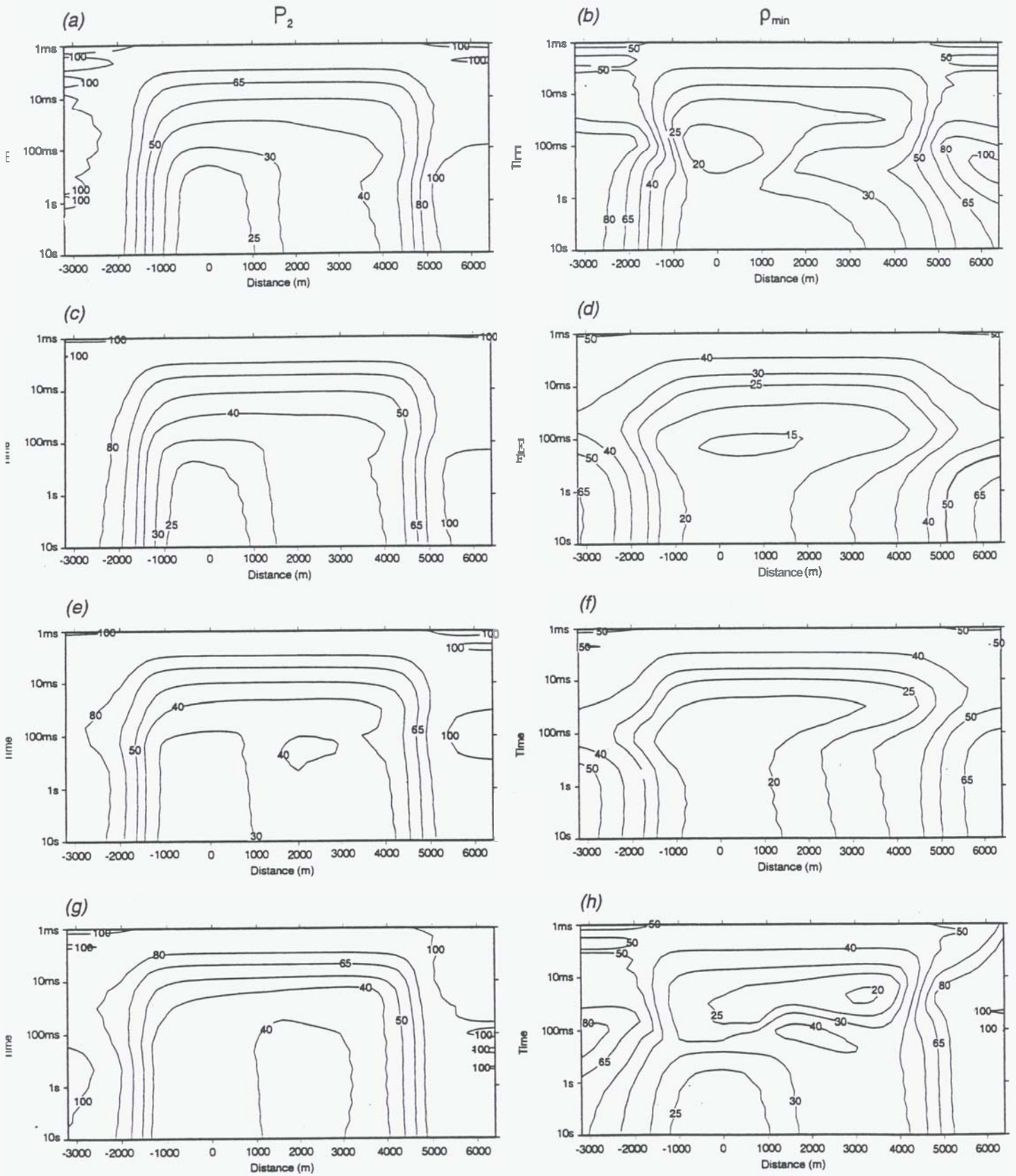


Figure 5. Pseudo sections for the instantaneous apparent resistivity tensor invariants  $P_2$  and  $\rho_{min}$  (in  $\Omega\cdot m$ ) for the 3D resistivity model shown in Fig. 4 along line A-A'. The results for each of the four different sources, S1 to S4, are shown as pairs ( $P_2$  and  $\rho_{min}$ ) in (a) & (b) to (g) & (h) respectively.



## CONCLUSIONS

The tensor formulation we have developed enables the TEM fields from more than one source polarisation to be analysed in terms of apparent resistivities that are, for idealised dipole current sources, independent of the orientation of the transmitter bipoles. The instantaneous apparent resistivity tensor retains many of the useful properties of the **DC** tensor particularly when the subsurface resistivity distribution is 3D. Our modelling results suggest that profiles of LOTEM measurements across 3D structures can be **used** to create an image of a 3D structure that reproduces the main features of **the** subsurface resistivity directly from the field data. By using the different invariants it is possible to take advantage of the all information contained in the multiple source **data**. The different invariants can be used to emphasise different aspects of the structure. Where the **LOTEM** data is not confined to a profile but is distributed over the target area, maps showing the apparent resistivity ellipses at different times can be made into a sequence of images which provide a dramatic way of visualising the tensor data.

The ultimate goal of any **EM** exploration survey is to **determine as far as** is possible the subsurface resistivity structure from the observed data. Increasingly, **2D** and **3D** inversion algorithms are being used for **this** purpose. In principle, the inversion procedures could be applied directly to the observed data. However, there are practical reasons for converting the measured data into an apparent resistivity. In particular, the apparent resistivity is a normalised parameter which assists the numerical stability of the inversion algorithm. More importantly the apparent resistivity data can be **used** to provide an unbiased starting model required by such schemes. If the apparent resistivity is a good approximation to the subsurface resistivity distribution then both the speed and robustness of the inversion scheme will be enhanced. The properties of the instantaneous apparent resistivity tensor and the need to use different source polarisations in 3D situations make the tensor formulation ideally suited for use with 3D inversion procedures.

## ACKNOWLEDGMENTS

Zonghou Xiong and Alan Tripp at the University of **Utah** made their **3D** modelling code available to **us** without which much of **this** work would not have been possible. Our **thanks** also go to George Risk for the many discussions we have had about the nature of the transient electric fields.

## REFERENCES:

- Bibby, H.M., 1977: The apparent resistivity tensor. *Geophysics* **42**, 1258-1261.
- Bibby, H.M., 1978: Direct current resistivity modeling for axially symmetric bodies using the finite element method. *Geophysics*, **4**, 550-562.
- Bibby, **H.M.**, 1986: **Analysis** of multiple source bipole-quadrupole resistivity surveys using the apparent resistivity tensor. *Geophysics*, **51**, 972-983.
- Bibby, H.M., 1994: Reply to comment on 'Three dimensional interpretation of multiple source bipole-dipole data using the apparent resistivity tensor.' by X.li and L.B.Pedersen. *Geophysical Prospecting*, **51**, 972-983.
- Bibby, H.M., and Hohmann, **G.W.**, 1993: Three dimensional interpretation of multiple source bipole-dipole data using the apparent resistivity tensor. *Geophysical Prospecting*, **41**:697-723.
- Caldwell, **T.G.** and Bibby, H.M., 1993: A comparison of electromagnetic methods with the **DC** resistivity multiple-source bipole-dipole method for deep geothermal exploration. Proc. 15th New Zealand Geothermal Workshop, 25-30.
- Pellerin, L., Johnston, J.M., and Hohmann, **G.W.**, 1992: Evaluation of electromagnetic methods in geothermal exploration. Expanded Abstracts with Biographies, 1992 Technical Program, Society of Exploration Geophysicists Sixty-Second Annual International Meeting, New Orleans, 405-408.
- Risk, **G.F.**, Bibby, H.M., and Caldwell, **T.G.**, 1993: **DC** resistivity mapping with the multiple-source bipole-dipole array in the central volcanic region, New Zealand. *J. Geomag. Geoelectr.*, **45**, 897-916.
- Risk, **G.F.**, Caldwell, **T.G.** and Bibby, **H.M.**, 1994: Deep resistivity surveys in the Waiotapu-Waikite-Reporoa region, New Zealand. *Geothermics* **23**:423-443
- Spies, **B.R.** and Frischknecht, **F.C.**, 1991: Electromagnetic sounding in electromagnetic methods in applied geophysics. Volume 2, applications. Editor **M.N.** Nabigian Society of Exploration Geophysicists, Tulsa.
- Strack K.M., 1991: German deep transient EM systems in electromagnetic methods in applied geophysics. Volume 2, applications. Editor M.N. Nabigian Society of Exploration Geophysicists, Tulsa.
- Strack **K.M.**, 1992: A practical review of deep transient electromagnetic exploration. Elsevier, Amsterdam.
- Xiong, **Z.**, 1992: Electromagnetic modelling of three-dimensional structures by the method of system iteration using integral equations. *Geophysics*, **57**, 1556-1561.
- Xiong, Z. and Tripp, A., 1995: A block iterative algorithm for 3-D electromagnetic modelling using integral equations with symmetrized substructures. *Geophysics*, **60**, 291-295.